Received: 3 February 2023 | Accepted: 8 February 2023

DOI: 10.1002/prp2.1071

ORIGINAL ARTICLE

The influence of SARS-CoV-2 infection on expression of drug-metabolizing enzymes and transporters in a hACE2 murine model

Kiran Deshpande[1,2] | Keith R. Lange[3] | William B. Stone[4] | Christine Yohn[1,2] | Naomi Schlesinger[5] | Leonid Kagan[1,2] | Albert J. Auguste[4,6] | Bonnie L. Firestein[3] | Luigi Brunetti[1,2]

[1]Department of Pharmaceutics, Ernest Mario School of Pharmacy, Rutgers, The State University of New Jersey, Piscataway, New Jersey, USA

[2]Center of Excellence in Pharmaceutical Translational Research and Education, Ernest Mario School of Pharmacy, Rutgers, The State University of New Jersey, Piscataway, New Jersey, USA

[3]Department of Cell Biology and Neuroscience, Rutgers, The State University of New Jersey, Piscataway, New Jersey, USA

[4]Department of Entomology, College of Agriculture and Life Sciences, Fralin Life Science Institute, Virginia Polytechnic Institute and State University, Virginia, USA

[5]Division of Rheumatology, Department of Medicine, Rutgers Robert Wood Johnson Medical School, New Brunswick, New Jersey, USA

[6]Center for Emerging, Zoonotic, and Arthropod-borne Pathogens, Virginia Polytechnic Institute and State University, Blacksburg, Virginia, USA

Correspondence
Luigi Brunetti, Pharmacy Practice and Pharmaceutics, 160 Frelinghuysen Road, Piscataway, NJ 08854, USA.
Email: luigi.brunetti@rutgers.edu

Funding information
IDCare

Abstract

Severe acute respiratory syndrome coronavirus 2 (SARS-CoV-2) infection and the resulting Coronavirus disease 2019 emerged in late 2019 and is responsible for significant morbidity and mortality worldwide. A hallmark of severe COVID-19 is exaggerated systemic inflammation, regarded as a "cytokine storm," which contributes to the damage of various organs, primarily the lungs. The inflammation associated with some viral illnesses is known to alter the expression of drug-metabolizing enzymes and transporters. These alterations can lead to modifications in drug exposure and the processing of various endogenous compounds. Here, we provide evidence to support changes in the mitochondrial ribonucleic acid expression of a subset of drug transporters (84 transporters) in the liver, kidneys, and lungs and metabolizing enzymes (84 enzymes) in the liver in a humanized angiotensin-converting enzyme 2 receptor mouse model. Specifically, three drug transporters (Abca3, Slc7a8, Tap1) and the pro-inflammatory cytokine IL-6 were upregulated in the lungs of SARS-CoV-2 infected mice. We also found significant downregulation of drug transporters responsible for the movement of xenobiotics in the liver and kidney. Additionally, expression of cytochrome P-450 2f2 which is known to metabolize some pulmonary toxicants, was significantly decreased in the liver of infected mice. The significance of these findings requires further exploration. Our results suggest that further research should emphasize altered drug disposition when investigating therapeutic compounds, whether re-purposed or new chemical entities, in other animal models and ultimately in individuals infected with SARS-CoV-2. Moreover, the influence and impact of these changes on the processing of endogenous compounds also require further investigation.

Abbreviations: Abc, ATP binding cassette family; ACE2, angiotensin-converting enzyme 2; cDNA, complementary deoxyribonucelic acid; COVID-19, Coronavirus disease 2019; Cyp, cytochrome P-450; DPI, days post-infection; IL, Interleukin; mRNA, mitochondrial ribonucleic acid; OATP, organic anion-transporting polypeptide; SARS-CoV-2, severe acute respiratory syndrome coronavirus 2; Slc, solute carrier family; Tap, transporter associated with antigen processing; TNF, tumor necrosis factor.

KEYWORDS
COVID-19, drug transporters, drug-metabolizing enzymes, hACE2, SARS-CoV-2

1 | INTRODUCTION

Coronaviruses are enveloped positive-strand RNA viruses, accounting for 10% to 30% of upper respiratory tract infections globally.[1] These viruses have long been considered inconsequential and a frequent cause of the common cold. This presumption has been challenged in contemporary times, with outbreaks of severe acute respiratory syndrome coronavirus (SARS-CoV), Middle East respiratory syndrome coronavirus, and recently, SARS-CoV-2 (Severe acute respiratory syndrome coronavirus 2). Infection with SARS-CoV-2, and its associated coronavirus disease 2019 (COVID-19), came to the forefront in late 2019, leading to unprecedented worldwide morbidity and mortality.

SARS-CoV-2 infection is characterized by an exaggerated inflammatory response, leading to the sequelae seen in COVID-19. The mechanism of SARS-CoV-2 viral entry into the cells is similar to that of SARS-CoV but with a higher specificity due to stronger hydrophobic interactions and salt bridge formation, causing increased pathogenicity.[2] Viral entry into cells leads to an immune response that triggers pneumonia and multiple organ failure due to cytokine-induced inflammation in severe cases. The increased circulation of pro-inflammatory substances observed during a cytokine storm is deemed the putative precipitating event that leads to many complications observed in patients with COVID-19. Individuals with severe COVID-19 often have other risk factors (i.e., diabetes, obesity) that may further contribute to the degree of systemic inflammation present. Inflammation contributes to a host of alterations in normal physiology, including changes in the expression of drug transporters and metabolizing enzymes. Similarly, Middle East respiratory infection induces inflammation, although delayed in onset,[3] and has been shown to alter drug transporters and metabolizing enzymes. SARS-CoV-2 gains entry to its host via the lungs and may infect other tissues that express ACE-2 such as the liver, kidneys, and brain.[4] Previous studies have identified increased serum interleukin (IL) concentrations in the patients with severe COVID-19.[5,6] Viral infections influence the expression of cytokines in the organs expressing ACE-2 and the resulting inflammation may alter drug metabolism.[7–9] While some have speculated that SARS-CoV-2 infection alters drug exposure and the risk for drug interactions, this concern has not garnered enough attention and certain aspects remain unstudied.

Understanding whether COVID-19 alters drug disposition and host physiological conditions via altered transporter and metabolizing enzymes is essential for unraveling disease mechanisms and the safe use of therapeutics. Given the potential for drug–drug and drug-disease interactions in individuals infected with SARS-CoV-2, it is paramount to identify which transporters and metabolizing enzymes are influenced by SARS-CoV-2 infection. The current study aims to identify drug transporters that may be altered in the lungs, kidneys, and liver and drug-metabolizing enzymes in the liver of a hACE2 (humanized angiotensin-converting enzyme 2) murine model.

Significance Statement

Infection with SARS-CoV-2 results in significant dysregulation of several drug transporters in the lungs, liver, and kidney. The impact of this dysregulation on drug disposition requires further study in alternative animal models of SARS-CoV-2 infection.

2 | MATERIALS AND METHODS

2.1 | Animal model

Adult hACE2 male mice (hACE2 on a C57BL/6J background) were purchased from The Jackson Laboratory and a colony maintained at Virginia Tech. The mice were separated into two groups, including SARS-CoV-2 challenge ($n = 10$; 5 mice were used for necropsy and 5 to monitor survival) and phosphate-buffered saline (PBS; $n = 5$) unchallenged healthy controls. Mice were challenged intranasally in each nare with 10^5 plaque-forming units (PFU) of SARS-CoV-2 (strain WA1/2020) or PBS diluent. After challenge, mice were monitored for weight change, signs of disease, and mortality for 6 days. Necropsies were conducted on 4–5 days post-infection (DPI), and tissues (i.e., liver, kidney, lung, brain, heart, and spleen) collected and stored in culture medium (i.e., Dulbecco's Modified Eagle Medium (DMEM) containing 2% Fetal Bovine Serum (FBS), 100 units of penicillin, and 0.1 mg streptomycin), for virus quantification by plaque assay on Vero-E6 cells as previously described[10] and RNA isolation. Plasma samples were not collected. Mice were immediately euthanized when moribund or upon weight loss greater than or equal to 20% of their original body weight, as previously described.[11,12]

2.2 | RNA isolation

Tissues were homogenized using a Qiagen Tissuelyser II (Qiagen, Hilden). Samples were clarified by centrifugation at 8000 × *g* for 5 min, 250 μL of supernatant was collected, and total RNA extracted using TriReagent (Thermo Fisher Scientific.) following the manufacturer's protocol. RNA was eluted in 30 μL of nuclease-free water. RNA was stored at −80°C until cDNA (Complementary deoxyribonucelic acid) synthesis.

2.3 | cDNA synthesis

On the day of assay, total RNA concentration was measured by Nanodrop 2000 Spectrophotometer (Thermo Fisher Scientific). Concentrated samples were diluted with nuclease-free water, and 1 μg of RNA was used for each reaction. cDNA was synthesized using the RT2 first strand kit (Qiagen Cat: 330404.). GE buffer (2 μL) was added to each 1 μg RNA sample, and the final volume was adjusted to 10 μL using Nuclease-Free Water (not DEPC-Treated, Ambion Cat: AM9937). DNAse elimination mix (80 μL; Qiagen Cat: 79254) was added to each sample before being incubated for 5 min at 42°C on a heat block and then placed on ice immediately. Once samples were kept on ice for at least a minute, they were used to synthesize cDNA. A mix of BC3 buffer, control P2 and RNAse-free water, and reverse transcriptase (10 μL) was added to the 10 μL volume containing GE Buffer, 1 μg RNA, and Nuclease-Free Water. This reaction was prepared in PCR thin-walled tubes and placed on ice, followed by a thermal cycler reaction (Bio-Rad C-1000 Touch Thermal cycler) for 42°C for 15 min. The reaction was immediately stopped by incubating at 95°C for 5 min, followed by placement on ice for at least 1 min. Then 20 μL of cDNA mix was diluted using 91 μL of Nuclease-Free Water (not DEPC-Treated, Ambion Cat: Cat: AM9937) to obtain a final volume of 111 μL reaction volume.

2.4 | RT-qPCR

RT-qPCR single-plex panels provided by Qiagen were used to assess drug transporter expression in the mouse lung, liver, and kidney samples. The expression of drug metabolizing enzymes was only measured in the liver samples (Qiagen Drug transporter GeneGlobe ID - PAMM-070ZC-24 Cat:330231 and Drug Metabolism I GeneGlobe ID - PAMM-068ZC-12 Cat:330231) (Table S2). Arrays were predesigned for a Step One Plus instrument (Applied Biosystems Cat: 4376600). RT^2 SYBR Green ROX qPCR Mastermix hot start *Taq* polymerase (Qiagen Cat: 330523) was used as the fluorescence dye. The reaction for the plate was prepared according to the manufacturer's protocol. Wells were configured with precoated target genes (84 wells) and housekeeping genes (5 wells), as well as mouse gDNA control (GDC), Positive PCR (PPC), and Reverse Transcription (RTC) controls. Before loading the plate, it was briefly centrifuged for 1 min to ensure no bubbles remained in the wells. The plate was then run on the RT-qPCR (StepOne software v2.2.2) using the recommended cycling conditions; 10 min 95°C one cycle and the 40 cycles at 95°C for 15 and 60°C for 1 min.

The quality of cDNA synthesized was assessed using the mouse genomic DNA (gDNA) control. The threshold set for the analysis was 0.2, and the baseline was taken between 3 and 15 cycles. Post analysis, the data were checked for mice GDC control and the positive PCR control and reverse transcriptase control (RTC) (at cutoff Ct 35). Undetermined gene expression values were assigned a Ct value of 35 to reduce bias in software calculations.[13] For the PCR control (PPC), the values were between Ct 18-to-22, and reverse transcription control (RTC) values were between Ct 13-to-27. If the data passed the criteria, they were uploaded to the GeneGlobe Data Analysis Center (available from: https://geneglobe.qiagen.com/us/analyze) for analysis. After comparing and confirming that controls were within range for Ct 35 cutoff, PPC Ct 18 to 22, and RTC Ct 13- 27 data were normalized to the 5 housekeeping genes (Gapdh, Actb, B2m, Gusb, Hsp90ab1). Target genes with more than three samples with undetermined or Ct > 35 values were manually removed from the analysis. Fold change values were calculated by the GeneGlobe software by normalizing the experimental group (SARS-CoV-2^+ mice) (2^[-$\Delta\Delta C_T$]) values to the control group (SARS-CoV-2^- mice) (2^[-$\Delta\Delta C_T$]) values.

To assess pro-inflammatory cytokines, single-plex RT-qPCR was run to analyze IL-6, TNF-α, and IL-1β. For these plates, each well consisted of 10 μL TaqMan Fast Advanced Mastermix (ThermoFisher 4444557), 1 μL control or target FAM TaqMan Probe, 7 μL Nuclease-Free water, and 2 μL cDNA sample. Before selecting a house-keeping gene, we analyzed the stability of the 5 house-keeping genes from the panels above with their respective TaqMan probe. We determined that Gapdh (ThermoFisher Taqman Assay Mm99999915_g1) was the most stable across tissues and samples. Quantitative PCR was performed in duplicate reactions, with target genes IL-6 (ThermoFisher Taqman Assay Mm00446190_m1), TNF-α (ThermoFisher Taqman Assay Mm00443258_m1) and IL-1β (ThermoFisher Taqman Assay Mm00434228_m1) and Gapdh on a StepOne Plus Real-Time PCR system (Applied Biosystems). Data were analyzed using the $\Delta\Delta C_T$ method, duplicate cycle thresholds per gene per sample were averaged, normalized to the control gene (Gapdh) to obtain ΔC_T, and were then converted to $\Delta\Delta C_T$ values by normalizing to mean ΔC_T's of the control group. Fold-change was then calculated and reported normalizing the experimental group (SARS-CoV-2^+ mice) (2^(-$\Delta\Delta C_T$)) values to the control group (SARS-CoV-2^- mice) (2^(-$\Delta\Delta C_T$)) values.

2.5 | Western blot analysis

Western blot analysis was performed if a significant fold-change in drug transporters or metabolizing enzyme gene expression was observed between infected versus non-infected animals in the PCR analysis with a preference on the lung tissue results. Protein from tissue extracts was resolved in SDS-polyacrylamide gels (NuPAGE™ 4 to 12%, Bis-Tris, 1.5 mm, Mini Protein Gels; ThermoFisher cat# NP0336PK2) at 115 V for 1.5 h. Proteins were then transferred to nitrocellulose membrane at 20 V for 1 h at room temp using 1X NuPAGE Transfer Buffer (ThermoFisher cat# NP00061) containing 10% methanol. The membrane was dried and then washed twice with deionized water. The membrane was incubated with 5 mL of REVERT protein stain (Li-Cor, cat# 103546–310) for 5 min with rocking at room temperature, washed twice with 5 mL of Revert WASH buffer (6.7% glacial acetic in 30%v/v methanol) and then imaged in the 700 nm channel using Licor Odyssey software to measure the total protein per well for normalization according to the manufacturer's protocol. Membranes were washed with Revert Destain solution (0.1 M NaOH, 30% methanol), followed by a wash with 1 X Tris-buffered saline

(TBS; Fisher cat # BP24711). Membranes were blocked in 1 X TBS+ 5% bovine serum albumin +0.02% sodium azide (block), incubated with indicated primary antibodies (Table S2) in block, washed 4 times in 1X TBS containing 0.1% Tween® 20 (TBST), and incubated with a secondary antibody (IRDYE 680RD) donkey anti-mouse IgG (Li-Cor cat# 926-68072) or IRDYE 800cw goat anti-rabbit IgG (Li-Cor cat# 926-32211) in block at 1:10000 dilution. Membranes were washed 4 times in 1X TBST and once with 1X TBS. Blots were images in the 700 and 800 channels using Licor Odyssey software.

2.6 | Data analysis

All data were analyzed using descriptive statistics in Graphpad Prism (version 9.3.1, San Diego, CA). Data were checked for potential outliers using Grubbs' test and examined for irregularities or missing values. Differences in gene (RT-qPCR; fold change) and protein (Western blot analysis; normalized to total protein) expression between SARS-CoV-2+hACE2 infected (experimental) and uninfected (control) mice were assessed using an independent sample *t*-test with $p<0.05$ as the threshold for significance. Data were normalized by log10 transformation when necessary and data distribution and variance was evaluated for normality. Data were analyzed using two-way ANOVAs followed by an ad hoc using Tukey's test where appropriate.

3 | RESULTS

3.1 | Animal model

hACE2 mice were intranasally inoculated with SARS-CoV-2 or PBS diluent. Mice began showing signs of illness at approximately 4 DPI, and symptoms worsened rapidly until euthanasia. Signs of disease included lethargy, hunched posture, and sunken eyes, eventually leading to paralysis and unresponsiveness. SARS-CoV-2 challenged mice showed rapid weight loss starting at 4 DPI (Figure 1A) and succumbed to infection by 6 DPI (Figure 1B) with 100% mortality. Infected mice also presented significant virus loads in the brain (~10^6 PFU/g) and lung (~10^5 PFU/g) tissues, and no virus was detected in the heart, liver, kidney, or spleen tissues sampled (Figure 1C).

4 | DRUG TRANSPORTER AND METABOLIZING ENZYME GENE EXPRESSION

Some degree of dysregulated gene expression was observed in the lungs, liver, and kidneys of SARS-CoV-2 infected mice versus controls (Figure 2). Changes in each tissue is summarized in the sections below.

4.1 | Lung drug transporter gene expression is upregulated in SARS-CoV-2 + hACE2 mice

The expression of drug transporters in lungs harvested from SARS-CoV-2 infected and uninfected hACE2 mice was analyzed (Figure 3). Infection of SARS-CoV-2 in hACE2 mice resulted in significant upregulation in the expression of three transporters: Abca3 ($t(8) = 3.336$, $p = 0.01$; SARS-CoV-2$^+$: M = 3.21, SD = 1.3; SARS-CoV-2$^-$: M = 1.11, SD = 0.54), Slc7a8a ($t(8) = 4.108$, $p = 0.003$; SARS-CoV-2$^+$: M = 2.82, SD = 0.75; SARS-CoV-2$^-$: M = 1.11, SD = 0.55), and Tap1 ($t(8) = 2.558$, $p = 0.034$; SARS-CoV-2$^+$: M = 4.776, SD = 3.22; SARS-CoV-2$^-$: M = 1.07, SD = 0.4). Western blot analysis demonstrated no change in protein levels of SLC22A8 (undetected), TAP1 ($p = 0.47$), and SLC22A2 ($p = 0.38$) (Table 1, Figure 3, Figure S1, and Table S1).

4.2 | Liver drug transporter and metabolizing enzyme gene expression are downregulated in SARS-CoV-2+ hACE2 mice

The expression of drug transporter and metabolizing enzyme genes was measured in liver tissue harvested from infected and uninfected

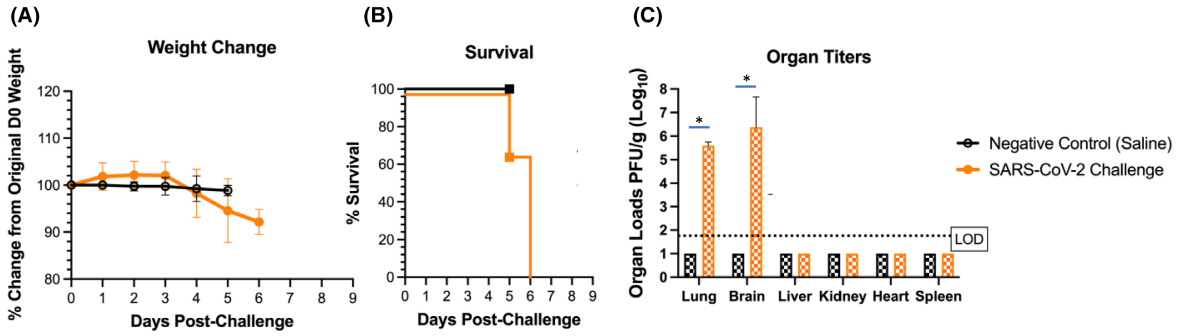

FIGURE 1 SARS-CoV-2 infection results in significant morbidity and mortality in adult hACE2 mice. Mice (PBS $n = 5$; SARS-CoV-2 $n = 10$) were challenged intranasally with 10^5 plaque-forming units (PFU) of virus in each nare, and (A) weight change and (B) survival measured daily post challenge. (C) Organ loads were measured 4 days post-infection for lung, brain, spleen, kidney, liver, and heart. Each data point plotted represents the mean values and error bars indicate standard deviation. The limit of detection (LOD) is indicated with a dotted line. Statistical significance is denoted as $^*p<0.05$.

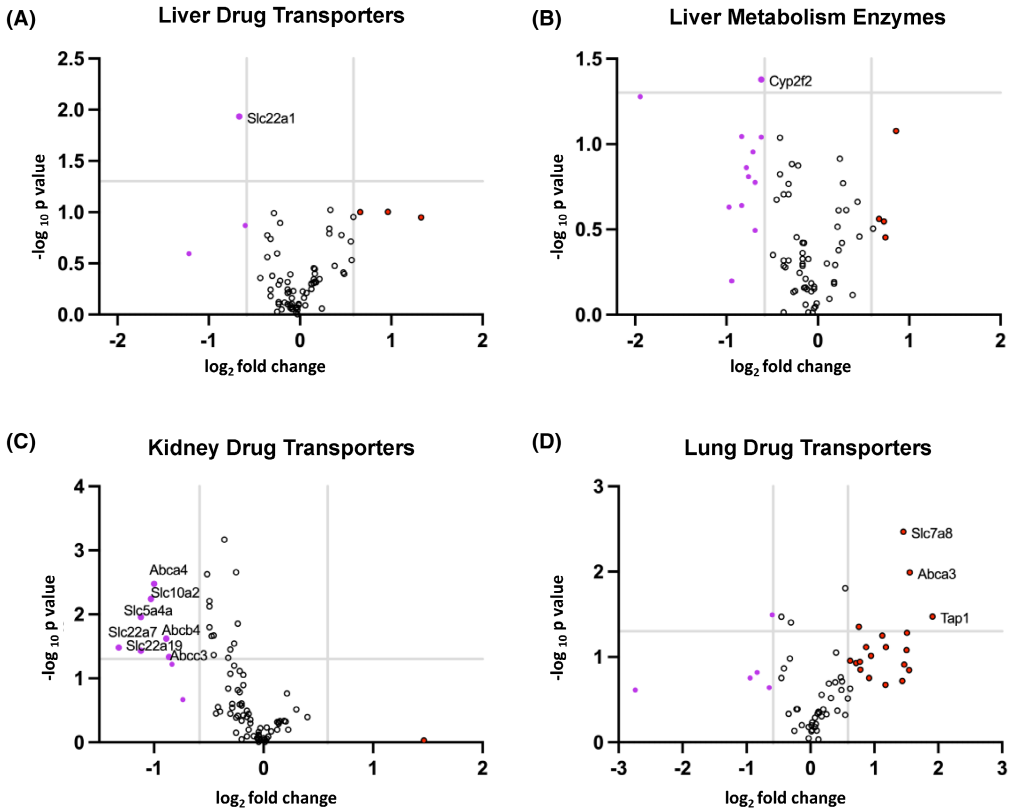

FIGURE 2 Volcano plots depicting SARS-CoV-2 induced changes in expression of drug transporters and metabolizing enzymes in tissues of infected relative to uninfected hACE2 mice. Adult hACE2 mice were treated with 10^5 PFU of SARS-CoV-2 (+) ($n = 5$) or with PBS (–) ($n = 5$), and tissues (liver, kidney, and lung) were isolated at 4/5 days post-infection. mRNA was isolated from tissues and underwent cDNA synthesis for RT-qPCR single plex panels provided by Qiagen. Target genes with more than 3 samples with undetermined or Ct > 35 values were manually removed from the analysis. Fold change values were calculated by the GeneGlobe software by normalizing the experimental group (SARS-CoV-2^+ mice) (2^(-$\Delta\Delta C_T$)) values to the control group (SARS-CoV-2^- mice) (2^(-$\Delta\Delta C_T$)) values. Log2 of fold changes was plotted against their statistical significance, with genes downregulated (purple dots) and upregulated (red dot). Distribution of liver drug transporters (A), liver metabolizing enzymes (B), kidney drug transporters (C), and lung drug transporters (D). Significant genes altered by SARS-CoV-2 infection are labeled in each graph.

hACE2 mice. The mRNA (mitochondrial ribonucleic acid) expression of drug transporter Slc22a1 (t (8) = 3.27, p = 0.0112) was significantly downregulated in the liver of infected (M = 0.64, SD = 0.19) compared to uninfected hACE2 mice (M = 1.01, SD = 0.17) (Table 2; Figure 4). In terms of metabolizing enzymes, cytochrome P450, family 2, subfamily f, polypeptide 2 (Cyp2f2) mRNA levels in infected hACE2 mice (M = 0.686, SD = 0.22) were significantly lower in expression than control mice (M = 1.02, SD = 0.22; t(8) = 2.398, p = 0.043) (Table 2; Figure 4).

4.3 | Kidney drug transporter gene expression is downregulated in SARS-CoV-2+ hACE2 mice

We analyzed the impact of SARS-CoV-2 on kidney drug transporter expression (Figure 4) and determined that the regulation of seven genes was significantly altered in infected hACE2 mice compared to uninfected mice (Table 2). SARS-CoV-2 infection caused the following transporters to be downregulated in the kidney: Abca4 (t(8) = 4.121, p = 0.0033; SARS-CoV-2^+: M = 0.51, SD = 0.12; SARS-CoV-2^-: M = 1.024, SD = 0.25), Abcb4 (t(8) = 2.773, p = 0.024; SARS-CoV-2^+: M = 0.59, SD = 0.26; SARS-CoV-2^-: M = 1.02, SD = 0.23), Abcc3 (t(8) = 2.346, p = 0.047; SARS-CoV-2^+: M = 0.58, SD = 0.2; SARS-CoV-2^-: M = 1.08, SD = 0.44), Slc10a2 (t(8) = 3.73, p = 0.0058; SARS-CoV-2^+: M = 0.53, SD = 0.2; SARS-CoV-2^-: M = 1.02, SD = 0.22), Slc22a19 (t(8) = 2.5, p = 0.0369; SARS-CoV-2^+: M = 0.51, SD = 0.31; SARS-CoV-2^-: M = 1.06, SD = 0.39), Slc22a7 (t(8) = 2.572, p = 0.033; SARS-CoV-2^+: M = 0.46, SD = 0.28; SARS-CoV-2^-: M = 1.09, SD = 0.47), and Slc5a4 (t(8) = 3.292, p = 0.011; SARS-CoV-2^+: M = 0.48, SD = 0.17; SARS-CoV-2^-: M = 1.05, SD = 0.34) (Figure 4). These genes downregulated by SARS-CoV-2 infection are important for transporting endogenous compounds (i.e., creatine), toxins, anionic drugs (i.e., NSAIDs), and xenobiotics in the kidney. Western blot analysis revealed that SLC5a4a (p = 0.33) and SLC10a2 (ASBT, p = 0.086) protein levels did not significantly change upon infection (Table 2, Figure 4).

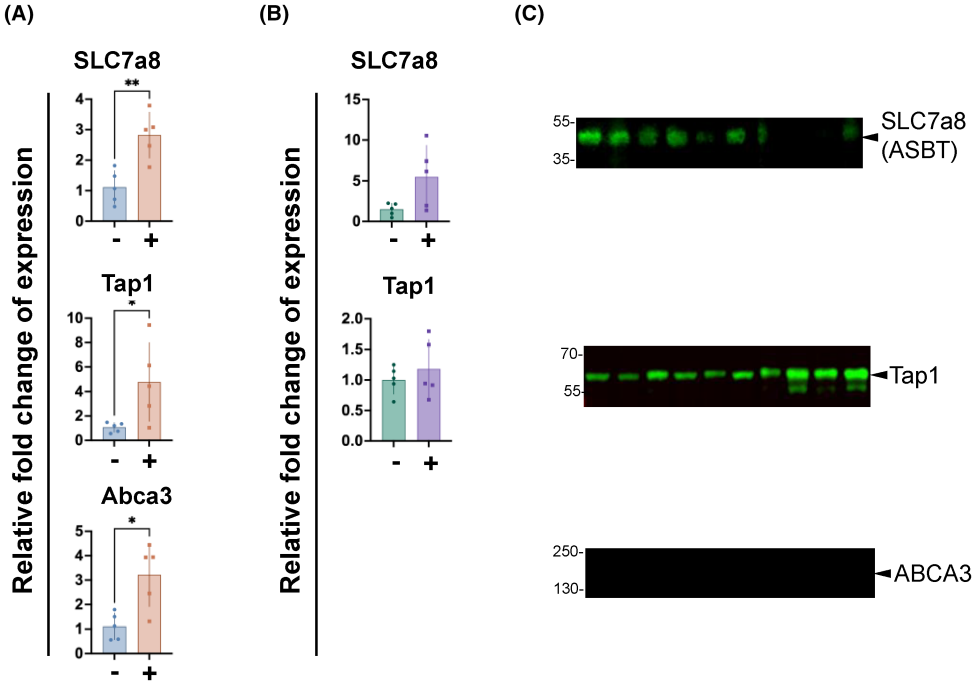

FIGURE 3 Infection with SARS-CoV-2 significantly upregulates mRNA expression of drug transporters in the lungs of hACE2 mice. (A) Lungs harvested from SARS-CoV-2+ hACE2 and SARS-CoV-2- hACE2 mice were analyzed by RT-qPCR for expression of drug transporters, with SLC7a8, Tap1, and Abca3 significantly upregulated in infected mice. (B) Quantitation of Western blots in panel C. (C) Images of quantified blots indicate similar protein expression between the groups. Blots were imaged with near-infrared fluorescence secondary antibodies (800CW Goat anti-Rabbit IgG), and bands were normalized to total protein (Figure S3). Quantification of individual bands was performed in Image Studio. Fold changes in expression were calculated using the average fluorescence of the PBS-treated group. $^{*}p<0.05$, $^{**}p<0.01$ as determined by Student's *t*-test.

TABLE 1 Significant changes in drug transporters and pro-inflammatory cytokine IL-6 gene expression in lungs of SARS-CoV-2 positive hACE2 mice compared to control mice.

Gene Symbol	Fold Change	*p* value	Function and potential relevance to SARS-CoV-2 pathophysiology
Abca3	3.21	0.01	Plasma membrane of alveolar type II cells, efflux transporter.[14] Regulation of pulmonary surfactant homeostasis; dysfunction linked to a variety of pulmonary diseases.[15]
Slc7a8	2.82	0.003	Glutamine efflux transporter,[16] SARS-CoV-2 requires glutamine for replication.[17] While not specifically studied in lung tissue Slc7a8 may have a role in mediating the release of glutamine in brain, liver, and skeletal muscle.[18]
Tap1	4.77	0.034	Peptide from cytoplasm to ER.[19,20] Upregulation enhances viral replication.[21]
IL-6	6.79	0.045	Interleukin-6 (IL-6) is produced in response to viral infections damaging tissues.[22] Angiotensin II is increased in SARS-Cov-2+ individuals, which can also increase IL-6 mRNA in a dose-dependent manner.[23] Elevated IL-6 levels (>80 pg/mL) has been used to identify SARS-Cov-2+ individuals with a high risk of respiratory failure.[24]

4.4 | IL-6 gene expression is upregulated in SARS-CoV-2 + hACE2 infected mice

Gene expression of IL-6, IL-1β, and TNF-α was measured using single-plex RT-qPCR with TaqMan Fast Advanced Mastermix and TaqMan probes per target gene in the lung, liver, and kidney. IL-6 expression in the lung of SARS-CoV-2+ hACE2 mice (M = 6.79, SD = 5.12) was significantly upregulated compared to uninfected mice (M = 1.25, SD = 1.03 $t(8) = 2.377$, $p = 0.0447$) (Figure S2). Western blot analysis revealed undetectable IL-6 expression in the lung (Figure S2). In

TABLE 2 Significant changes in drug transporters (liver and kidney) and drug metabolizing enzymes (liver) gene expression in SARS-CoV-2 positive hACE2 mice versus control mice.

Gene Symbol	Tissue	Fold Change	*p* value	Function and potential relevance to SARS-CoV-2 pathophysiology
Slc22a1	Liver	0.644	0.0112	Organic cation transporter-1 (OCT-1), transport of commonly used medications such as metformin.[25] Remdesivir inhibits OCT-1.[26]
Cyp2f2	Liver	0.686	0.043	Enzyme is mainly expressed in the liver, but in mice also found in the respiratory tract[27] where it metabolizes pulmonary toxicants and procarcinogens.[28] Following exposure to peroxisome proliferators (plasticizer DEHP) CYP2f2 is reduced in mouse livers.[29]
Abca4	Kidney	0.51	0.0033	Removes N-retinylidene-PE, from photoreceptor cells following transduction in the retina.[30] Role in kidney not defined.
Abcb4	Kidney	0.59	0.024	Translocates phosphatidylcholine (PC) from the inner to the outer leaflet of the canalicular membrane of the hepatocyte.[31] Role in kidney not defined.
Slc10a2	Kidney	0.53	0.0058	Apical sodium-dependent bile acid transporter (ASBT); related to the development of hepatobiliary, inflammatory bowel, and metabolic diseases.[32] Role in kidney not defined.
Slc5a4a	Kidney	0.48	0.011	Selective inhibitors of sodium-glucose cotransporter 3 (SGLT-3) serves as a sodium transporter.[33] This transporter also function as a glucose sensor.[34]
Abcc3	Kidney	0.58	0.047	Efflux transporter expressed in liver, intestine, adrenal gland, pancreas, hepatocytes and kidney.[35]
Slc22a19	Kidney	0.51	0.0369	Encodes for organic anion transporter 5 (OAT5) and is expressed exclusively in the kidney. Oat5 permits the transport of endogenous compounds, toxins, and anionic drugs (i.e. NSAIDs). It is a proposed biomarker for renal damage: prerenal (induced by vascular calcification) and intrarenal (induced by nephrotoxic agents).[36]
Slc22a7	Kidney	0.46	0.033	Encoded for organic anion transporter 2 (OAT2), with expression in both liver and kidney.[37] In the kidney OAT2 facilitates creatine transport,[38] with xenobiotics like cobicistat increasing serum creatine.

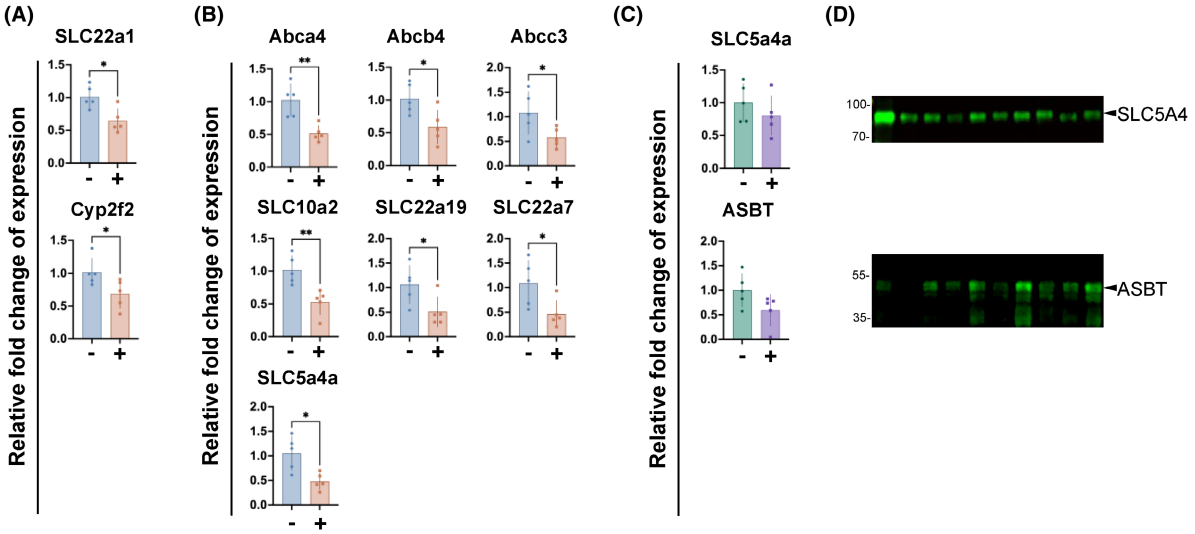

FIGURE 4 Infection with SARS-CoV-2 significantly downregulates mRNA expression of drug transporters in the liver and kidney and a liver metabolic enzyme in hACE2 mice. (A) Liver harvested from SARS-CoV-2+ hACE2 and SARS-CoV-2- hACE2 was analyzed by RT-qPCR for expression of drug transporters and metabolizing enzymes. The drug transporter SLC22a1 and metabolizing enzyme (Cyp2f2) were significantly downregulated in infected hACE2 mice compared to hACE2 uninfected mice. (B) Kidneys from hACE2 mice infected with SARS-CoV-2 compared to uninfected mice had significant downregulation in the expression of Abca4, Abcb4, Abcc3, SLC10a2 (ASBT), SLC22a19, SLC22a7, and SLC5a4a. (C) Quantitation of Western blots in panel D. Protein levels were not different between infected and uninfected hACE2 mice for SLC5a4a and ASBT (SLC10a2). (D) Imaged Blots were imaged with near-infrared fluorescence secondary antibodies (800CW Goat anti-Rabbit IgG), and bands were normalized to total protein (Figures S4-S6). Quantification of individual bands was performed in Image Studio. Fold changes in expression were calculated using the average fluorescence of the PBS-treated group. $^{*}p<0.05$, $^{**}p<0.01$as determined by Student's *t*-test.

the liver and kidney, IL-6 gene and protein levels were unaltered by SARS-CoV-2 infection. Additionally, in all tissues, gene and protein expression of both IL-1β and TNF-α were not significantly different between infected and uninfected mice (Figure S2).

5 | DISCUSSION

Dissecting the impact of SARS-CoV-2 on the interplay between IL-6 and drug transporters in the lung is important in advancing our understanding of how SARS-CoV-2 infection impacts the pathogenesis, drug disposition, and therapeutic efficacy response for the patient. We identified significant upregulation of three drug transporters (Abca3, Slc7a8, Tap1) and the pro-inflammatory cytokine IL-6 in the lungs of SARS-CoV-2 infected hACE2 mice. Mounting evidence suggests dysregulated drug transporter expression in the lung may influence drug exposure and influence the severity of illness.[39,40] The liver and kidney are commonly considered when investigating how disease states impact drug metabolizing enzymes and transporters, and ultimately drug disposition. We found significant downregulation of multiple drug transporters in the liver and kidney that are important for transporting xenobiotics. Moreover, the expression of the drug-metabolizing enzyme Cyp2f2, reported to be expressed in mouse lung and respiratory tract[27] was significantly decreased in the liver of infected mice. These findings have significant implications for drug development, drug dosing, and decoding the mechanisms of SARS-CoV-2 pathogenicity.

The lung is the primary organ affected by SARS-CoV-2 infection, and our analyses identified significant changes in the expression of Abca3, Slc7a8, and Tap1 in SARS-CoV-2 infected hACE2 mice. Changes to these transporters are observed in pulmonary diseases and viral infections (Table 1). Dysfunction in the efflux transporter Abca3 is observed in pulmonary diseases as this gene is important for regulating pulmonary surfactant homeostasis.[15] One molecule crucial for SARS-CoV-2 replication is glutamine.[17] Slc7a8, is a known efflux transporter of glutamine with expression in various tissues, including the lungs.[16] While not explicitly studied in lung tissue, Slc7a8 may have a role in mediating the release of glutamine in the brain, liver, and skeletal muscle.[18] The upregulation of this transporter during infection, as we observed, may be a mechanism by which SARS-CoV-2 meets glutamine demand for viral replication. Another means by which SARS-CoV-2 may replicate is via increased expression of Tap1,[21] which we observed in the lungs of infected mice. Inflammation due to SARS-CoV-2 infection may increase the expression of these transporters that promote viral replication, as IL-6 was upregulated in the lungs of infected mice. IL-6 is produced in response to viral infections that damage tissues,[22] with the lung being the main organ implicated in SARS-CoV-2 pathogenesis. Herold et al.[24] found that circulating levels of IL-6 can be used to identify individuals with COVID-19 at risk for respiratory failure.[24]

The liver is a major organ for metabolism and infection-related inflammation may lead to altered gene expression (Deb, Arrighi, and pharmacokinetics 2021; Li, Fan, and Hepatology 2020). In addition, the liver is a key organ involved in drug disposition, and inflammation in this organ can influence the risk-to-benefit ratio of drugs via altered drug transporter and metabolizing enzyme expression. IL-1, IL-6, and tumor necrosis factor-alpha (TNF-alpha) are the primary inflammatory cytokines that trigger an acute immune response. During SARS-CoV-2 infection, IL-6 is produced by macrophages and is often elevated.[41] Elevated TNFα and IL-6 levels downregulate mRNA expression of the organic anion-transporting polypeptide OATP1B1, OATP1B3, OATP2B1, organic cation transporter OCT1, and organic anion transporter 2 OAT2F in primary hepatocytes.[42] IL-6 suppresses the expression of a variety of cytochrome P-450 enzymes, including isoenzyme 3A4, the most abundantly expressed enzyme in this class,[43] in multiple in vitro and in vivo models.[44] P-glycoprotein expression was decreased in hepatic cell lines and mice after exposure to IL-6.[45,46] In the current study, we found a significant >1.5-fold downregulation in Slc22a1 gene expression. Notably, a significant increase in IL-6 gene expression was not identified in the liver and may explain the lack of changes in drug transporters in the liver.

Acute kidney injury is a common finding in patients infected with SARS-CoV-2; this comorbidity is associated with significant tissue inflammation.[47,48] Of the transporters with a significant change in gene expression identified in this study, Slc5a4a, Abcc3, Slc22a19, and Slc22a7 have physiological roles in the normal kidney. The human orthologue for Slc5a4a encodes the sodium-glucose cotransporter 3 (SGLT3),[33] which functions as a glucose sensor and does not transport glucose across the cell membrane.[49] In an LPS-induced inflammation murine model of sepsis and acute kidney injury, elevated pro-inflammatory cytokines were associated with the downregulation of SGLT3.[50] Blood glucose concentration is a significant prognostic predictor in patients with COVID-19, and those with elevated glucose levels >6.1 mmol/L have a 58% higher risk for disease progression, and 3.22-fold increased mortality risk.[51] Whether downregulation of this gene contributes to the glucose dysregulation observed in SARS-CoV-2 infection remains to be investigated. Slc22A7 and Slc22a19 encode Oat2 and Oat5, respectively. These genes were significantly downregulated in SARS-CoV-2 infected hACE2 mice. Both are responsible for transporting xenobiotics, endogenous compounds, and toxins.[36,37] Oat2 substrates include salicylate, acetylsalicylate, prostaglandin E2, dicarboxylates, glutamate, and some antivirals.[52] Interestingly, as discussed above, glutamine is required for SARS-CoV-2 replication.[17]

A vital consideration in the interpretations of our findings is the selection of animal models.[53,54] The ideal model for investigating SARS-CoV-2 infection has yet to be identified and each model has its inherent limitations. In the hACE2 murine model, a previous report suggests that SARS-CoV-2 viral replication and histopathological evidence of organ damage occur in the lung; however, viral antigen was not detected in the kidneys or liver.[55] Moreover, there was no histopathological evidence of inflammatory cells in these organs. This limitation may have influenced the ability of the animal model used in the current study to capture the extent of changes to gene expression of drug metabolizing and transporters induced

by SARS-CoV-2 infection. This limitation may explain the inability of the current findings to translate mRNA alterations to associated protein expression changes in the kidney and liver (Deb, Arrighi, and pharmacokinetics 2021). However, our primary goal was to investigate the alterations in drug transporters in the lungs. ACE2 receptors are primarily expressed in the lungs in both mice and humans; therefore, the changes observed in the hACE2 murine model for lung recapitulate the human condition (Hamming et al. 2004). Further studies to confirm these results in another animal model such as hamsters or non-human primates are necessary.

The differences in mRNA and protein expression results may reflect a time course of changes after infection. Analysis was performed 4 to 5 DPI, and there may have been a peak or trough of protein expression that followed changes to mRNA levels that may have occurred prior to this time. It is also possible that although mRNA expression changed at this point, changes to protein levels may lag due to either degradation of protein or translation of nascent protein. Future studies will include a more comprehensive time course of mRNA considering the functional changes and effect on drug absorption, distribution, metabolism and excretion of drugs and protein expression post-infection.

It should be noted that changes to mRNA gene expression changes did not completely overlap with changes to protein expression levels after infection in the hACE2 mouse model. This observation may be due to the performance of assays in tissue collected at one time point after infection. For example, it is possible that changes to mRNA levels precede changes to protein. Furthermore, we did not assess whether the localization of proteins changed in response to infection. Drug transporters may be internalized from the plasma membrane,[56,57] and Western blot analysis of total protein does not take this into account. Based on these caveats, our study should be repeated as a time course to assay both mRNA and protein levels. Additionally, immunohistochemistry or subcellular fractionation should be used to assess alterations in the membrane localization of drug transporters. Finally, repeat of experiments with larger numbers of animals will enhance the power of the study.

Nonetheless, our findings are essential for understanding how drug disposition may be altered during infections that incite excessive inflammation. Drug transporters in lung disposition are understudied and must be considered when developing SARS-CoV-2 therapeutics since this is the primary target tissue. This consideration is crucial as novel therapeutics emerge, including those directly delivered to the lungs via inhalation or nebulization. Moreover, our findings should be considered when the hACE2 murine model is used for evaluating drug efficacy or toxicity.

6 | CONCLUSIONS

Based on the current study, there is a change in gene expression for drug transporters in the lungs, potentially altering therapies used to target COVID-19 and associated ailments. The changes in drug metabolism and transporters observed in the liver and kidney may also alter drug–drug interactions, eventually leading to an ineffective or toxic regimen. Implementing models that accurately reflect the disease condition in humans will aid in the development of therapies that reduce future potential organ toxicity and worsening symptoms. Thus, the current study lays the foundation for identifying the changes in expression of drug metabolism enzymes and drug transporters in response to COVID-19, emphasizing a detailed assessment of drug-disease interaction to improve patient health and avoid long-term side effects.

AUTHOR CONTRIBUTIONS

Participated in research design: Brunetti, Deshpande, Firestein, Lange, Auguste, Stone, Yohn. Conducted experiments: Deshpande, Lange, Auguste, Stone, Yohn. Contributed new reagents or analytical tools: Brunetti, Firestein, Auguste, Stone. Performed data analysis: Brunetti, Deshpande, Lange, Auguste, Stone, Yohn. Wrote or contributed to the writing of the manuscript: Deshpande, Lange, Stone, Yohn, Schlesinger, Kagan, Auguste, Firestein, Brunetti.

ACKNOWLEDGMENTS

The authors wish to acknowledge IDCare of Hillsborough for their generous funding to support the purchase of all required antibodies and assays. We would also like to acknowledge Drs. Tamara Minko, Ah-Ng Kong and Arash Hatefi for providing us to use the Applied Biosystems Step One Plus, Bio-Rad C-1000 Touch Thermal cycler and Nanodrop 2000 Spectrophotometer respectively.

FUNDING INFORMATION

This work was partially supported by grants from the National Institute of Allergy and Infectious Diseases of the National Institutes of Health under Award Number R01AI153433 to AJA. This work was also supported by a USDA National Institute of Food and Agriculture, Hatch VA160103, project 1020026, and a seed grant from the College of Agriculture and Life Sciences at Virginia Tech.

DATA AVAILABILITY STATEMENT

The data that support the findings of this study are available from the corresponding author, LB, upon reasonable request.

DISCLOSURE

The authors report no relevant conflicts of interest.

ORCID

Luigi Brunetti https://orcid.org/0000-0003-0565-6167

REFERENCES

1. Paules CI, Marston HD, Fauci AS. Coronavirus infections—more than just the common cold. *JAMA*. 2020;323:707-708.
2. Shang J, Ye G, Shi K, et al. Structural basis of receptor recognition by SARS-CoV-2. *Nature*. 2020;581:221-224.
3. Lau SKP, Lau CCY, Chan KH, et al. Delayed induction of proinflammatory cytokines and suppression of innate antiviral response by the novel Middle East respiratory syndrome

coronavirus: implications for pathogenesis and treatment. *J Gen Virol*. 2013;94:2679-2690.
4. Hamming I, Timens W, MLC B, et al. Tissue distribution of ACE2 protein, the functional receptor for SARS coronavirus. A first step in understanding SARS pathogenesis. *J Pathol Soc*. 2004;203:631-637.
5. Deb S, Arrighi S. Potential effects of COVID-19 on cytochrome P450-mediated drug metabolism and disposition in infected patients. *Eur J Drug Metab*. 2021;46:185-203.
6. Chen T, Wu D, Chen H, et al. Clinical characteristics of 113 deceased patients with coronavirus disease 2019: retrospective study. *BMJ*. 2020b;368:m1091.
7. Lenoir C, Terrier J, Gloor Y, et al. Impact of SARS-CoV-2 infection (COVID-19) on cytochromes P450 activity assessed by the Geneva cocktail. *Clin Pharmacol Ther*. 2021;110:1358-1367.
8. Chen Q, XuL, DaiY, et al. Cardiovascular manifestations in severe and critical patients with COVID-19. *Clin Cardiol*. 2020a;43:796-802.
9. Li J, Fan J-G. Characteristics and mechanism of liver injury in 2019 coronavirus disease. *J Clin Transl Hepatol*. 2020;8:13-15.
10. Coria LM, Saposnik LM, Pueblas Castro C, et al. A novel bacterial protease inhibitor adjuvant in RBD-based COVID-19 vaccine formulations containing alum increases neutralizing antibodies, specific germinal center B cells and confers protection against SARS-CoV-2 infection in mice. *Front Immunol*. 2022;13:844837.
11. Lopez K, Wilson SN, Coutermash-Ott S, et al. Novel murine models for studying Cache Valley virus pathogenesis and in utero transmission. *Emerg Microbes Infect*. 2021;10:1649-1659.
12. Porier DL, Wilson SN, Auguste DI, et al. Enemy of my enemy: a novel insect-specific Flavivirus offers a promising platform for a Zika virus vaccine. *Vaccines (Basel)*. 2021;9:1142.
13. McCall MN, McMurray HR, Land H, Almudevar A. On non-detects in qPCR data. *Bioinformatics*. 2014;30:2310-2316.
14. Fitzgerald ML, Xavier R, Haley KJ, et al. ABCA3 inactivation in mice causes respiratory failure, loss of pulmonary surfactant, and depletion of lung phosphatidylglycerols. *J Lipid Res*. 2007;48:621-632.
15. Beers MF, Mulugeta S. The biology of the ABCA3 lipid transporter in lung health and disease. *Cell Tissue Res*. 2017;367:481-493.
16. Bhutia YD, Ganapathy V. Glutamine transporters in mammalian cells and their functions in physiology and cancer. *Biochim Biophys Acta*. 2016;1863:2531-2539.
17. Bharadwaj S, Singh M, Kirtipal N, Kang SG. SARS-CoV-2 and glutamine: SARS-CoV-2 triggered pathogenesis via metabolic reprograming of glutamine in host cells. *Front Mol Biosci*. 2020;7:627842.
18. Pochini L, Scalise M, Galluccio M, Indiveri C. Membrane transporters for the special amino acid glutamine: structure/function relationships and relevance to human health. *Front Chem*. 2014;2:61.
19. Behar SM, Dascher CC, Grusby MJ, Wang C-R, Brenner MB. Susceptibility of mice deficient in CD1D or TAP1 to infection with mycobacterium tuberculosis. *J Exp Med*. 1999;189:1973-1980.
20. Korkolopoulou P, Kaklamanis L, Pezzella F, Harris AL, Gatter KC. Loss of antigen-presenting molecules (MHC class I and TAP-1) in lung cancer. *Br J Cancer*. 1996;73:148-153.
21. Xia Z, Xu G, Yang X, et al. Inducible TAP1 negatively regulates the antiviral innate immune response by targeting the TAK1 complex. *J Immunol*. 2017;198:3690-3704.
22. Rose-John S, Scheller J, Elson G, Jones SA. Interleukin-6 biology is coordinated by membrane-bound and soluble receptors: role in inflammation and cancer. *J Leukoc Biol*. 2006;80:227-236.
23. Funakoshi Y, Ichiki T, Ito K, Takeshita A. Induction of interleukin-6 expression by angiotensin II in rat vascular smooth muscle cells. *Hypertension*. 1999;34:118-125.
24. Herold T, Jurinovic V, Arnreich C, et al. Elevated levels of IL-6 and CRP predict the need for mechanical ventilation in COVID-19. *J Allergy Clin Immunol*. 2020;146:128-136.
25. Goswami S, Gong L, Giacomini K, Altman RB, Klein TE. PharmGKB summary: very important pharmacogene information for SLC22A1. *Pharmacogenet Genomics*. 2014;24:324-328.
26. Ambrus C, Bakos E, Sarkadi B, Ozvegy-Laczka C, Telbisz A. Interactions of anti-COVID-19 drug candidates with hepatic transporters may cause liver toxicity and affect pharmacokinetics. *Sci Rep*. 2021;11:17810.
27. Li L, Wei Y, Van Winkle L, et al. Generation and characterization of a Cyp2f2-null mouse and studies on the role of CYP2F2 in naphthalene-induced toxicity in the lung and nasal olfactory mucosa. *J Pharmacol Exp Ther*. 2011;339:62-71.
28. Hukkanen J, Pelkonen O, Hakkola J, Raunio H. Expression and regulation of xenobiotic-metabolizing cytochrome P450 (CYP) enzymes in human lung. *Crit Rev Toxicol*. 2002;32:391-411.
29. Ye X, Lu L, Gill SS. Suppression of cytochrome P450 Cyp2f2 mRNA levels in mice by the peroxisome proliferator diethylhexylphthalate. *Biochem Biophys Res Commun*. 1997;239:660-665.
30. Tsybovsky Y, Molday RS, Palczewski K. The ATP-binding cassette transporter ABCA4: structural and functional properties and role in retinal disease. *Adv Exp Med Biol*. 2010;703:105-125.
31. Oude Elferink RP, Paulusma CC. Function and pathophysiological importance of ABCB4 (MDR3 P-glycoprotein). *Pflugers Arch*. 2007;453:601-610.
32. Yang N, Dong YQ, Jia GX, et al. ASBT(SLC10A2): a promising target for treatment of diseases and drug discovery. *Biomed Pharmacother*. 2020;132:110835.
33. Kothinti RK, Blodgett AB, North PE, Roman RJ, Tabatabai NM. A novel SGLT is expressed in the human kidney. *Eur J Pharmacol*. 2012;690:77-83.
34. Bianchi L, Diez-Sampedro A. A single amino acid change converts the sugar sensor SGLT3 into a sugar transporter. *PLoS One*. 2010;5:e10241.
35. Scheffer GL, Kool M, de Haas M, et al. Tissue distribution and induction of human multidrug resistant protein 3. *Lab Invest*. 2002;82:193-201.
36. Campagno RV, Nosetto EC, Brandoni A, Torres AM. Utility of urinary organic anion transporter 5 as an early biomarker of obstructive nephropathy. *Clin Exp Pharmacol Physiol*. 2020;47:1674-1681.
37. Cropp CD, Komori T, Shima JE, et al. Organic anion transporter 2 (SLC22A7) is a facilitative transporter of cGMP. *Mol Pharmacol*. 2008;73:1151-1158.
38. Lepist EI, Zhang X, Hao J, et al. Contribution of the organic anion transporter OAT2 to the renal active tubular secretion of creatinine and mechanism for serum creatinine elevations caused by cobicistat. *Kidney Int*. 2014;86:350-357.
39. Ehrhardt C, Backman P, Couet W, et al. Current Progress toward a better understanding of drug disposition within the lungs: summary proceedings of the first workshop on drug transporters in the lungs. *J Pharm Sci*. 2017;106:2234-2244.
40. Redente EF. ABC transporters: an overlooked mechanism of drug failure in our preclinical models? *Am J Respir Cell Mol Biol*. 2020;62:130-131.
41. Rubin EJ, Longo DL, Baden LR. Interleukin-6 receptor inhibition in Covid-19 - cooling the inflammatory soup. *N Engl J Med*. 2021;384:1564-1565.
42. Le Vee M, Lecureur V, Stieger B, Fardel O. Regulation of drug transporter expression in human hepatocytes exposed to the proinflammatory cytokines tumor necrosis factor-alpha or interleukin-6. *Drug Metab Dispos*. 2009;37:685-693.
43. Stavropoulou E, Pircalabioru GG, Bezirtzoglou E. The role of cytochromes P450 in infection. *Front Immunol*. 2018;9:89.
44. Kumar D, Trivedi N. Disease-drug and drug-drug interaction in COVID-19: risk and assessment. *Biomed Pharmacother*. 2021;139:111642.
45. Lee G, Piquette-Miller M. Influence of IL-6 on MDR and MRP-mediated multidrug resistance in human hepatoma cells. *Can J Physiol Pharmacol*. 2001;79:876-884.

46. Sukhai M, Yong A, Kalitsky J, Piquette-Miller M. Inflammation and interleukin-6 mediate reductions in the hepatic expression and transcription of the mdr1a and mdr1b genes. *Mol Cell Biol Res Commun*. 2000;4:248-256.
47. Fanelli V, Fiorentino M, Cantaluppi V, et al. Acute kidney injury in SARS-CoV-2 infected patients. *Crit Care*. 2020;24:155.
48. McWilliam SJ, Wright RD, Welsh GI, et al. The complex interplay between kidney injury and inflammation. *Clin Kidney J*. 2021;14:780-788.
49. Barcelona S, Menegaz D, Diez-Sampedro A. Mouse SGLT3a generates proton-activated currents but does not transport sugar. *Am J Physiol Cell Physiol*. 2012;302:C1073-C1082.
50. Schmidt C, Hocherl K, Bucher M. Regulation of renal glucose transporters during severe inflammation. *Am J Physiol Renal Physiol*. 2007;292:F804-F811.
51. Wang W, Shen M, Tao Y, et al. Elevated glucose level leads to rapid COVID-19 progression and high fatality. *BMC Pulm Med*. 2021;21:1-13.
52. Nigam SK, Bush KT, Martovetsky G, et al. The organic anion transporter (OAT) family: a systems biology perspective. *Physiol Rev*. 2015;95:83-123.
53. Casel MAB, Rollon RG, Choi YK. Experimental animal models of coronavirus infections: strengths and limitations. *Immune Network*. 2021;21:e12.
54. Pandey K, Acharya A, Mohan M, Ng CL, Reid SP, Byrareddy SN. Animal models for SARS-CoV-2 research: a comprehensive literature review. *Transbound Emerg Dis*. 2021;68:1868-1885.
55. Bao L, Deng W, Huang B, et al. The pathogenicity of SARS-CoV-2 in hACE2 transgenic mice. *Nature*. 2020;583:830-833.
56. Evers R, Piquette-Miller M, JW P, et al. Disease-associated changes in drug transporters may impact the pharmacokinetics and/or toxicity of drugs: a white paper from the international transporter consortium. *Clin Pharmacol Ther*. 2018;104:900-915.
57. Murray M, Zhou F. Trafficking and other regulatory mechanisms for organic anion transporting polypeptides and organic anion transporters that modulate cellular drug and xenobiotic influx and that are dysregulated in disease. *Br J Pharmacol*. 2017;174:1908-1924.

SUPPORTING INFORMATION

Additional supporting information can be found online in the Supporting Information section at the end of this article.

How to cite this article: Deshpande K, Lange KR, Stone WB, et al. The influence of SARS-CoV-2 infection on expression of drug-metabolizing enzymes and transporters in a hACE2 murine model. *Pharmacol Res Perspect*. 2023;11:e01071. doi:10.1002/prp2.1071